Effect of Cr, Mo, and Nb additions on intergranular cohesion of ferritic stainless steel: First-principles determination*

Li Chun-Xia(李春霞)[a)b)c)], Dang Sui-Hu(党随虎)[a)b)c)], Wang Li-Ping(王丽萍)[a)b)], Zhang Cai-Li(张彩丽)[a)b)], and Han Pei-De(韩培德)[a)b)†]

[a)] *Key Laboratory of Interface Science and Engineering in Advanced Materials of Ministry of Education, Taiyuan University of Technology, Taiyuan* 030024, *China*

[b)] *College of Materials Science and Engineering, Taiyuan University of Technology, Taiyuan* 030024, *China*

[c)] *College of Physics and Electronic Engineering, Yangtze Normal University, Chongqing* 408003, *China*

(Received 5 August 2013; revised manuscript received 2 September 2013; published online 12 February 2014)

Effects of Cr, Mo, and Nb on the ferritic stainless steel ∑(210) grain boundary and intragranularity are investigated using the first-principles principle. Different positions of solute atoms are considered. Structural stability is lowered by Cr doping and enhanced by Mo and Nb doping. A ranking on the effect of solute atoms enhancing the cohesive strength of the grain boundary, from the strongest to the weakest is Cr, Mo, and Nb. Cr clearly prefers to locate in the intragranular region of Fe rather than in the grain boundary, while Mo and Nb tend to segregate to the grain boundary. Solute Mo and Nb atoms possess a strong driving force for segregation to the grain boundary from the intragranular region, which increases the grain boundary embrittlement. For Mo- and Nb-doped systems, a remarkable quantity of electrons accumulate in the region close to Mo (Nb). Therefore, the bond strength may increase. With Cr, Mo, and Nb additions, an anti-parallel island is formed around the center of the grain boundary.

Keywords: first-principles principle, grain boundary cohesion, electronic properties, ferritic stainless steel

PACS: 71.15.Mb, 71.15.Nc, 71.20.Be, 73.20.At **DOI:** 10.1088/1674-1056/23/3/037102

1. Introduction

Stainless steel has been used in various applications due to many superior properties such as formability, strength, and corrosion resistance.[1–3] Ferritic stainless steels containing relatively small amount of Cr (10.5%–11.75%), e.g., 430 and 409 stainless steels, have been used mainly in automotive exhaust systems because they exhibit satisfactory corrosion resistance and cost less than other stainless steels containing large additions of alloying elements. However, the use of such low-Cr ferritic stainless steels is limited due to their high corrosion rate in aggressive environments. In addition to Cr, Mo and Nb can improve the corrosion resistance of heat-resistant ferritic stainless steels, which are used in high-temperature applications. In general, the corrosion resistance and mechanical properties of polycrystalline alloys depend on the cohesion at bulk interfaces of the crystal grains. Impurities and alloying elements affect the structure and properties of interfaces at the atomic level when they segregate to the grain boundary (GB). These impurities and alloying elements may either be detrimental or beneficial in GB cohesion. In this work, we explore the effect of a small amount of Cr, Mo, or Nb addition on the cohesive and electronic properties of GBs in Fe.

The composition and structure of a GB can be determined experimentally by high-resolution transmission electron microscopy and X-ray diffraction. However, to measure the interface thermodynamic quantities accurately is quite difficult. First-principles quantum-mechanical methods based on density functional theory (DFT) provide an appropriate tool to obtain reliable quantitative information on GB structure and energies at an electronic level. The DFT method has been successfully used to study the effect of solutes on interfacial strength in several systems. A good example for addressing this relation is the Rice–Wang theory.[4] Based on the Rice–Wang model, the properties of body-centered cubic (bcc) Fe Σ5 (210) GB with B, C, S, N, O, and P impurities were studied using different exchange–correlation density functions.[5,6] Moreover, impurity segregation and co-segregation at ∑13(111),[7–10] ∑5(310),[11,12] and ∑15(013)[13] GB in bcc Fe were studied using different theoretical methods.

Direct experimental observations[14,15] of Fe containing H, He, B, Sn, Sb, and S have also provided support for the Rice–Wang theory. Kin *et al.* studied the effect of vanadium on the strength of bcc Fe ∑3(111)[110] GB.[16] Results for ∑5(310) GB doped with Si and Sn have been reported.[17] The segregating effect of Nb and V on bcc Fe ∑3[110] (111) GB cohesion was studied via the DMol method. The results

*Project supported by the National Natural Science Foundation of China (Grant No. 51371123), the Specialized Research Foundation of the Doctoral Program for Institution of Higher Education of China (Grant No. 2013140211003), the Science and Technology Research Project of Municipal Education Commission of Chongqin, China (Grant Nos. KJ131308 and KJ131315), and the Natural Science Foundation of Science and Technology Commission of Chongqin, China (Grant No. cstc2012jjA90017).

†Corresponding author. E-mail: hanpeide@tyut.edu.cn

© 2014 Chinese Physical Society and IOP Publishing Ltd

showed that chemical and mechanical effects are crucial in determining whether a material is brittle or ductile.[18] The segregation effects of Co and Cr on bcc Fe ∑3[110] (111) GB cohesion were investigated via the DMol method. The results indicated that the segregation of Cr could improve GB cohesion.[19] As demonstrated by semi-empirical tight-binding calculations,[20] the ferromagnetism of Fe stabilizes intergranular cohesion. However, magnetism at Fe GB was not extensively explored in terms of first-principles principle. Variations in magnetic moments at the Fe GB were discussed for ∑5(210),[6] ∑5(310),[17] and ∑3(111).[21–23] More recently, the magnetic properties of tilt Fe GB for ∑3(111) and ∑5(210) with a small amount of Cr addition, were investigated through first-principles methods.[22,24] In all cases, the magnetic moments of the GB atoms exhibit an oscillatory variation with atomic layer depth, and show a decrease toward the bulk value.

To the best of our knowledge, no such studies dealing with the interface properties of dilute Fe–Nb (or Mo) ferritic stainless steels with high Fe content have been reported. The embrittling and strengthening effects of these alloying elements are still not well understood. In this work, we perform first-principles DFT calculations to obtain reliable quantitative information on the structure and energy of Fe interfaces at an electronic level. We address the effect of a low concentration of Cr, Mo, or Nb additions to the Fe host grains on the GB and intragranular cohesion. Our calculations allow us to gain insight into the microstructure, bonding, and strength at the Fe GB and their dependence on electronic and magnetic properties, which can be modified by a small amount of Cr, Mo, or Nb additions. Charge density distribution and calculated local density of states provide insight into the electronic environment of Fe atoms close to the GB, which deepens our understanding of the mechanics and magnetic properties at a microscopic level in ferritic stainless steel GBs with an alloying element.

2. Model and computation details

Our model of the ∑5 (210) tilt boundary uses a 70-atom unit cell with a large c cell parameter that runs perpendicularly to the GB, but has smaller dimensions in the other directions (see Fig. 1). The initial cell size is $5.73 \times 6.41 \times 21.77$ Å^3. Because of their large atomic size, Cr, Mo, and Nb will probably occupy the substitution site rather than the interstitial site on the GB or free surface (FS). In this work, we only consider the substitution case. To determine the preferred substitution position in the α-Fe GB, three cases (Case 1, Case 2, and Case 3) are considered, which correspond to Fe1, Fe10, and Fe11 atoms in Fig. 1 substituted by Cr, Mo, and Nb, respectively. Here, Case 1, Case 2, and Case 3 are considered as representatives to segregate from the interior of the grain to the GB for alloying elements Cr, Mo, and Nb. Case 1 represents alloying elements located at a site on the GB; Case 2 means alloying elements are close to the GB; and Case 3 means that alloying elements locate at the interior of the grain.

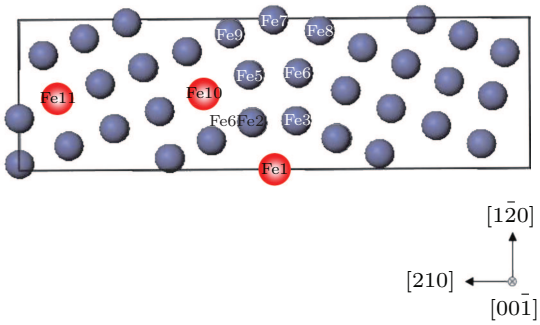


Fig. 1. (color online) Model of Fe with (210) tilt grain boundary. Three cases (Case 1, Case 2, and Case 3) are considered, which correspond to Fe1, Fe10, and Fe11 atoms substituted by an alloying element (Cr/Mo/Nb).

All our GB simulations have been conducted using density functional theory.[25,26] The calculations are conducted using the CASTEP code.[27] We used standard periodic boundary conditions with ultrasoft pseudopotentials[28] representing the core electrons and a plane-wave basis set representing the valance electrons. A plane-wave cutoff of 500 eV is found to be sufficient to make the total energy and the geometry structure of α-Fe converge. The K-point sampling during geometry optimization is carried out on a $2 \times 2 \times 1$ Monkhorst–Pack grid.[29] The Gaussian smearing parameter is 0.1 eV in width. The exchange–correlation interactions are treated using the spin-polarized version of the generalized gradient approximation within the scheme of Perdew–Burke–Ernzerhof (PBE).[30] All atomic positions are optimized in accordance with Hellman–Feynman forces until all the forces are less than 0.05 eV/Å.

3. Results and discussion

3.1. Binding energy and segregation energy

Binding energy E_b is used to compare the relative stability of the structure. It is defined as

$$E_b = E_{total} - \sum n_i \mu_i, \quad (1)$$

where E_{total} is the calculated total energy of the unit cell, n_i denotes the number of atomic species i (i = Fe, Cr, Mo, or Nb) in the unit cell, and μ_i is the atomic chemical potential.

The binding energy for various cases is illustrated in Fig. 2. In the calculations described here, it is assumed that the alloying elements are present inside the grain and locate on the GB. To determine the stability of the structure for alloying elements to segregate from the interior of the grain to the GB, additional calculations are performed. Regardless of Cr, Mo, or Nb doping, it can be seen that Case 1 (GB) has the lowest binding energy among the three cases, which corresponds to a more stable structure. Compared with a clean GB, the binding

energy is enhanced in Cr doping, while the structural stability is reduced. In contrast, the binding energies are reduced in Mo and Nb doping, while the stability is enhanced. The structural stability can be ordered in terms of decreasing E_b as follows: Nb-doped > Mo-doped > clean GB > Cr-doped.

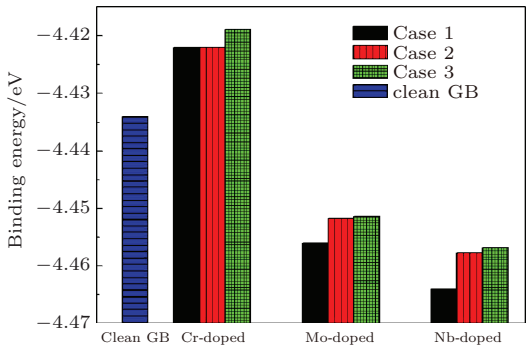


Fig. 2. (color online) Binding energies for clean, Cr-, Mo-, and Nb-doped Fe GB systems. Three cases (Case1, Case 2, and Case 3) are considered.

To determine the preferred site of alloying elements in Fe, the segregation energy is calculated, which is defined as the difference between the binding energies of the doped and the clean system. Here it is the energy in a typical GB environment; it can indicate the tendency of the alloying element to segregate into the GB. As a substitution atom, ΔE_{GB} is defined as

$$\Delta E_{GB} = E_b(GB + i) - E_b(GB), \tag{2}$$

where E_b(GB+i) and E_b(GB) indicate the binding energies of the GB system with the alloying element (Cr, Mo, or Nb) and clean GB, respectively. The calculated values of ΔE_{GB} are shown in Fig. 3. Cr clearly prefers to locate in the bulk Fe rather than in the GB. In Mo- and Nb-doped systems, the reversal of the sign of the ΔE_{GB}, particularly in Case 1, indicates a smaller negative value of ΔE_{GB}, which implies that Mo and Nb tend to segregate to the GB rather than to the interior of the grain. Furthermore, Nb is most likely to compete with other alloying elements for a site on the GB.

The segregation energies to the GB allow determination of the effect of impurity atoms on the cohesive strength of the GB. If it is negative, then the cohesive strength of the GB

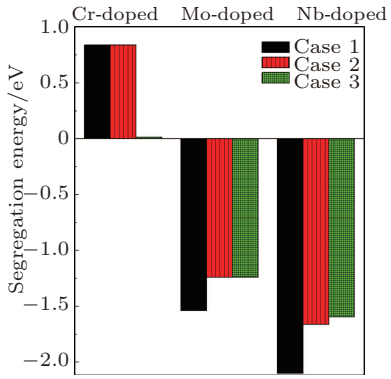


Fig. 3. (color online) Segregation energy for Cr-, Mo-, and Nb-doped Fe GB. Three cases (Case1, Case 2, and Case 3) are considered.

increases. If it is positive, then the GB is weakened. Figure 3, therefore, suggests that Mo and Nb should enhance the GB's resistance to decohesion, while Cr should weaken the GB.

3.2. Effects of alloying elements on Fe GB embrittlement

A thermodynamic theory developed by Rice and Wang,[31] based on the Griffith fracture theory,[4] describes the mechanism of interfacial embrittlement due to solute segregation, which is indicated by the competition between brittle interfacial separation and crack blunting. The degree of embrittlement can be predicted by

$$2\gamma_{int} \cong (2\gamma_{int})_0 - (\Delta g_b - \Delta g_s)\Gamma, \tag{3}$$

where $(2\gamma_{int})_0$ is the separation work of a clean interface, Γ is the concentration of segregants per unit area of the interface, Δg_b and Δg_s can be obtained from the segregation energies of the solute atoms towards the GB and FS which are ΔE_{GB} and ΔE_{FS}, respectively. If the solute atoms tend to segregate to the GB rather than the surface, then $\Delta E_{GB} - \Delta E_{FS} < 0$, and the solute atoms are considered as a cohesive enhancer. For $\Delta E_{GB} - \Delta E_{Fs} > 0$, they are considered as an embrittler.

In general, the effect of solute atoms on the GB can be classified into chemical and mechanical components. It is proposed that the process of GB fracture can be considered as two steps. First, the GB splits into two separate surfaces (SS) without any relaxation; the binding energy difference in this stage, $\Delta E_{GB} - \Delta E_{SS}$, is the chemical component. Then, the two separated surfaces are fully relaxed into a free surface and $\Delta E_{SS} - \Delta E_{FS}$ is the mechanical component.

All the mentioned quantities are calculated and the results are listed in Table 1. For Cr-, Mo-, and Nb-doped systems, the contributions of chemical components are −0.408, −0.066, and −0.254 eV, respectively. They are comparable to the corresponding mechanical components, which are 0.253, 0.171, and 0.456 eV, respectively. The negative values indicate that both chemical and mechanical effects are beneficial to the GB cohesion. Therefore, from the point of the chemical component, Cr, Mo, and Nb are GB cohesion enhancers to a rather different extent. In contrast, the mechanical component in Cr-, Mo-, and Nb-doped systems has a positive value and becomes the dominant factor, which reveals that the cracking of the GB into 2 FS's is energetically more favorable.

For Cr doping, the detrimental effect of the mechanical component is not strong enough to counteract its beneficial chemical effect. Because $\Delta E_{GB} - \Delta E_{FS} = -0.155$ eV, the net effect of Cr on the GB would enhance the cohesion of the GB. The calculation in Ref. [19] shows that Cr on α-Fe GB may enhance cohesion. Furthermore, the studies of Yang *et al.*[32,33] pointed out that Cr is a powerful element for enhancing the cohesion of the γ-iron GB. It appears that Cr can enhance the cohesion of the GB irrespective of whether it is a γ-Fe GB or an α-Fe GB.

Table 1. Calculated binding energy difference (in eV) for the grain boundary (ΔE_{GB}), unrelaxed free surface (ΔE_{SS}), and relaxed free surface (ΔE_{FS}) for clean GB and Cr-, Mo-, and Nb-doped GB systems.

	ΔE_{GB}	ΔE_{SS} unrelaxed	ΔE_{FS} relaxed	$\Delta E_{GB} - \Delta E_{SS}$ chemical comp.	$\Delta E_{SS} - \Delta E_{FS}$ mechanical comp.	$\Delta E_{GB} - \Delta E_{FS}$ total
Cr-doped	0.012	0.420	0.167	−0.408	0.253	−0.155
Mo-doped	−0.022	0.044	−0.127	−0.066	0.171	0.105
Nb-doped	−0.030	0.224	−0.232	−0.254	0.456	0.202

However, for Mo and Nb doping, the situations are rather different from that of Cr doping. The detrimental effect of the mechanical component seriously offsets the beneficial effect of the chemical component. The net effect in Mo-doped and Nb-doped GBs, i.e., $\Delta E_{GB} - \Delta E_{FS}$, are 0.105 eV and 0.202 eV, respectively, implying that Mo and Nb may facilitate the brittle fracture of the GB. Shang *et al.*[16] have also confirmed that Nb may facilitate the brittle fracture of the GB after considering the mechanical component. Furthermore, the detrimental effect of structural relaxation generally depends on the atomic volume difference between the doping atom and the host metal atom. Messmer *et al.*[34,35] proposed that a larger atom is a more potent embrittler than a smaller atom due to the strains produced by the doping atom in a matrix. It stands to reason that Mo and Nb cause detrimental effects due to their larger atomic radii (1.40 Å for Mo, 1.48 Å for Nb, 1.27 Å for Cr, and 1.26 Å for Fe).

3.3. Charge distribution, magnetism, and local density of states

In this section, we discuss the results of the charge distribution, magnetism, and local density of states (LDOS) for clean, Cr-, Mo-, and Nb-doped GB systems.

The charge density on the (210) plane ([120] direction) for clean, Cr-, Mo- and Nb-doped GB are shown in Fig. 4. Compared with the clean GB, Cr–Fe6 bonding is very similar to the Fe1–Fe6 bonding. Figure 4 also clearly shows the enhanced atom bonding of Fe2, Fe3, and Fe6 with Mo (Nb), because a remarkable quantity of electrons accumulates in the region between these atoms. These effects are mainly attributed to the charge transfer from a doped atom to its neighboring Fe atoms in different systems. To show this, we list the electron occupation number obtained by Mulliken population analysis in Table 2. It can be seen that the electron occupation numbers of the host atoms Fe2, Fe3, Fe6, Fe7, Fe8, and Fe9 increase when Fe1 is replaced by an Nb atom, indicating that the host atoms close to Nb acquire more electrons because more electrons surround them. Thus, the bond strength across the GB may increase. Compared with the Nb- and Mo-doped systems, when an Fe1 atom is replaced by a Cr atom, the host atoms Fe3 and Fe9 near the Cr atom acquire fewer electrons, Fe2, Fe6, and Fe7 lose electrons, and thus the bond strength across the GB may decrease. Therefore, the charge transfer between the alloying elements and the neighboring Fe atoms is responsible for the changes in cohesion at the GB. Meanwhile, an Fe1 atom loses electrons at the clean GB, and a Mo or Nb atom loses more electrons at a Mo- or Nb-doped GB (0.03 e at a clean GB, 0.69 e at a Mo-doped GB, and 1.55 e at a Nb-doped GB). However, for a Cr-doped system, a Cr atom loses 0.04 e near the clean GB.

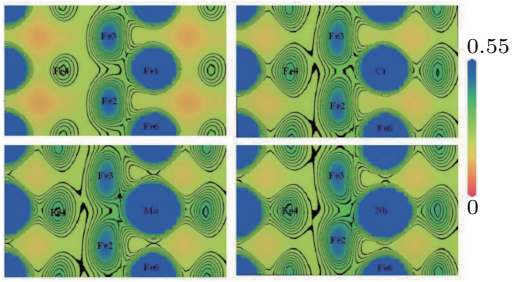


Fig. 4. (color online) Total valence charge density (in units of e/Å) on the (210) plane for the clean, Cr-, Mo-, and Nb-doped GB systems.

It is well known that bcc Fe exhibits ferromagnetism because of the exchange interaction. The values of atomic magnetic moments in clean GB are different from those for perfect bcc Fe (about $2.20\mu_B$ per atom), which is a result of different magnitudes of the 3d exchange splitting of Fe atoms in a clean GB. For a Mo- or Nb-doped system, it can be seen from Table 2 that the magnetic moments S of the neighboring Fe atoms decrease, which reveals that Mo (Nb) is a destroyer of magnetism for the host Fe atoms. In contrast, the magnetic moments of some host Fe atoms decrease and some increase in a Cr-doped system. Meanwhile, Cr, Mo, and Nb atoms exhibit different magnetic moments from that of bulk materials, but also unparallel to that of Fe1 atom in bcc Fe GB. In addition, an anti-parallel spin island is formed around the center of the GB in bcc Fe. The LDOS is obtained by broadening the discrete eigenvalue spectrum with a set of Lorentzian functions. The LDOS for some atoms of interest in clean GB, Cr-, Mo-, and Nb-doped GB are shown in Fig. 5. It can be educed that in the clean GB, Fe1, Fe3, Fe4, and Fe6 have close zero-system magnetic moments, corresponding to $-0.027\mu_B$, $-0.0536\mu_B$, $-0.0168\mu_B$, and $-0.0287\mu_B$, forming anti-ferromagnetic states. Compared with the clean GB, the host Fe3, Fe4, and Fe6 atoms in the Cr-, Mo-, and Nb-doped GB have the same magnetism (anti-ferromagnetic), but with different magnitudes. Unlike Fe1 atom, Cr, Mo, and Nb display ferromagnetism, and the magnetic moment is $-0.943\mu_B$, $-0.530\mu_B$, and $-0.561\mu_B$, respectively.

Table 2. Electron occupation number in the valence orbital and the net number of electrons $Q = N - Z_{\rm val}$. $Z_{\rm val}$ is the standard occupation number; N_0 and N are the orbital occupation numbers of clean GB and doped GB, respectively. The change $\Delta N = N - N_0$ and $\Delta Q = Q_{\rm gb+M} - Q_{\rm gb}$ (e) induced by the substitution of Cr, Mo, or Nb for an Fe1 atom is shown along with the magnetic moments S_0 (S) for each atom ($u_{\rm B}$) in clean GB (doped GB).

Atom		Clean GB		Cr-doped				Mo-doped				Nb-doped			
		N_0	S_0	N	S	ΔN	ΔQ	N	S	ΔN	ΔQ	N	S	ΔN	ΔQ
Fe1 (Cr/Mo/Nb)	s	0.67	–	2.74	–	–	–	2.76	–	–	–	2.66	–	–	–
	p	0.64	–	6.35	–	–	–	5.57	–	–	–	4.77	–	–	–
	d	6.64	–	4.87	–	–	–	4.98	–	–	–	4.03	–	–	–
	Q	−0.03	1.08	−0.04	−1.71	–	−0.01	−0.69	−0.59	–	−0.66	−1.55	−0.50	–	−1.52
Fe2	4s	0.68	–	0.73	–	0.05	–	0.75	–	0.07	–	0.78	–	0.10	–
	4p	0.72	–	0.61	–	−0.11	–	0.60	–	−0.12	–	0.62	–	−0.10	–
	3d	6.65	–	6.66	–	0.01	–	6.69	–	0.04	–	6.71	–	0.06	–
	Q	0.05	1.08	0.00	1.06	–	−0.05	0.04	0.90	–	−0.01	0.10	0.91	–	0.06
Fe3	4s	0.69	–	0.72	–	0.03	–	0.72	–	0.03	–	0.73	–	0.04	–
	4p	0.64	–	0.61	–	−0.03	–	0.62	–	−0.02	–	0.65	–	0.01	–
	3d	6.64	–	6.65	–	0.01	–	6.65	–	0.01	–	6.65	–	0.01	–
	Q	−0.03	1.14	−0.02	1.11	–	0.01	−0.01	1.10	–	0.02	0.03	1.08	–	0.06
Fe6	4s	0.63	–	0.61	–	−0.02	–	0.62	–	−0.01	–	0.65	–	0.02	–
	4p	0.74	–	0.67	–	−0.07	–	0.70	–	−0.04	–	0.73	–	−0.01	–
	3d	6.61	–	6.63	–	0.02	–	6.62	–	0.01	–	6.64	–	0.03	–
	Q	−0.01	1.21	−0.09	1.22	–	−0.08	−0.05	1.19	–	−0.04	0.01	1.16	–	0.02
Fe7	4s	0.68	–	0.70	–	0.02	–	0.74	–	0.06	–	0.79	–	0.11	–
	4p	0.73	–	0.68	–	−0.05	–	0.68	–	−0.05	–	0.69	–	−0.04	–
	3d	6.64	–	6.66	–	0.02	–	6.70	–	0.06	–	6.72	–	0.08	–
	Q	0.05	1.07	0.04	1.07	–	−0.01	0.12	0.88	–	0.07	0.2	0.91	–	0.15
Fe8	4s	0.66	–	0.61	–	−0.05	–	0.62	–	−0.04	–	0.64	–	−0.02	–
	4p	0.69	–	0.73	–	0.04	–	0.74	–	0.05	–	0.76	–	0.07	–
	3d	6.62	–	6.63	–	0.01	–	6.63	–	0.01	–	6.64	–	0.02	–
	Q	−0.03	1.18	−0.03	1.19	–	0.00	−0.01	1.14	–	0.02	0.04	1.14	–	0.07
Fe9	4s	0.65	–	0.70	–	0.05	–	0.74	–	0.09	–	0.78	–	0.13	–
	4p	0.74	–	0.70	–	−0.04	–	0.69	–	−0.05	–	0.70	–	−0.04	–
	3d	6.61	–	6.66	–	0.05	–	6.70	–	0.09	–	6.72	–	0.11	–
	Q	0.00	1.20	0.06	1.08	–	0.06	0.13	0.87	–	0.13	0.20	0.90	0.20	0.20

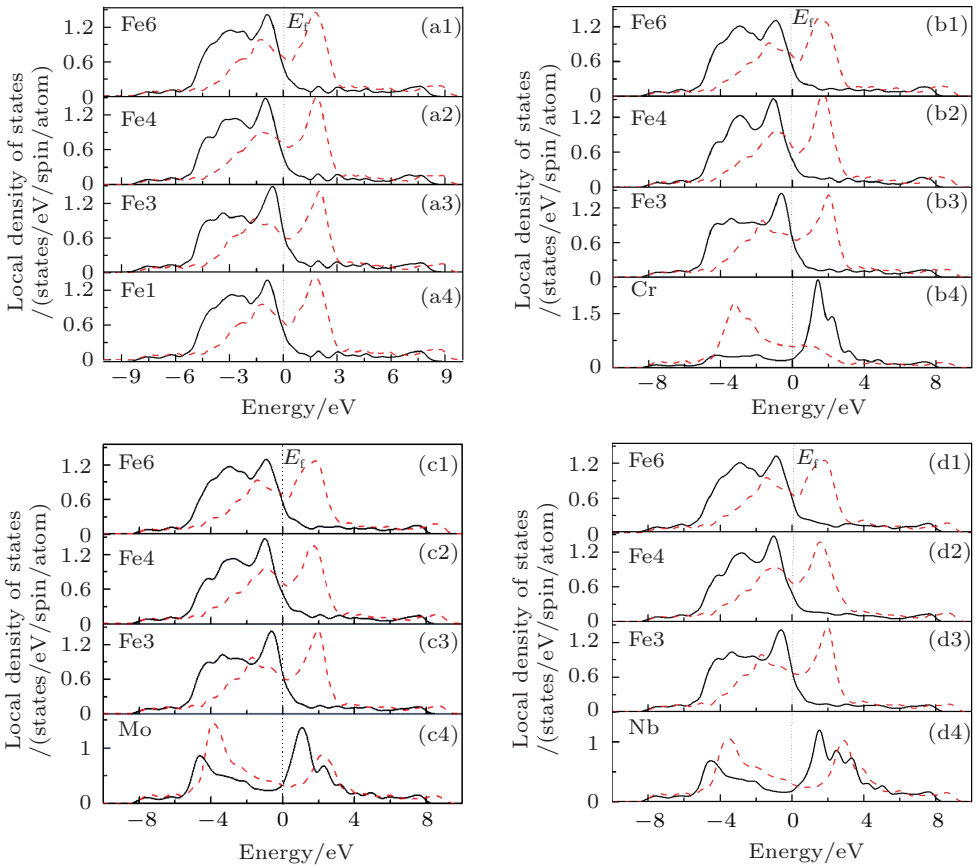


Fig. 5. (color online) Local densities of states are for Fe1/ (Cr, Mo, or Nb) and neighboring Fe3, Fe4, and Fe6 atoms in clean and doped GB systems. (a) Clean Fe GB; (b) Cr-doped Fe GB; (c) Mo-doped Fe GB; (d) Nb-doped Fe GB. The solid and dashed lines represent the LDOS of spin-up and spin-down states, respectively.

4. Conclusions

The effects of Cr, Mo, and Nb on the ferritic stainless steel ∑(210) GB and intragranular region are investigated from first principles. Results of binding energies, segregation energies, and interfacial embrittlement are presented. To determine the stability of structure for alloying elements to segregate from the interior of the grain to the GB, it is assumed that alloying elements are present inside the grain and locate on the GBs. Our calculations show that structural stability is reduced by Cr doping and enhanced by Mo and Nb doping. A ranking on the effect of solute atoms enhancing the cohesive strength of the grain boundary, from the strongest to the most weakest, is Cr, Mo, and Nb. Analysis of the segregation energy indicates that Cr clearly prefers to locate in the intragranular region of Fe rather than in the GB, while the solute atoms Mo and Nb have a strong driving force for segregation to the GB from the intragranular region, which increases the GB embrittlement. For Mo- and Nb-doped systems, a remarkable quantity of electrons accumulate in the region neighboring Mo (Nb), and the bond strength may increase. In addition, with Cr, Mo, and Nb additions, an anti-parallel spin island around the center of the GB in bcc Fe is formed.

References

[1] Amuda M O H and Mridha S 2012 *Mater. Design* **35** 609
[2] Hu J, Wang X P, Zhuang Z, Zhang T, Fang Q F and Liu C S 2013 *Chin. Phys. Lett.* **30** 046201
[3] Chung S K and Kyung Y J 2012 *Chin. Phys. Lett.* **29** 060702
[4] Rice J R and Wang J S 1989 *Mater. Sci. Eng. A* **107** 23
[5] Braithwaite J S and Rez P 2005 *Acta Mater.* **53** 2715
[6] Wachowicz E and Kiejna A 2008 *Comput. Mater. Sci.* **43** 736
[7] Fen Y Q and Wang C Y 2001 *Comput. Mater. Sci.* **20** 48
[8] Wang S Y, Wang C Y and Zhao D L 2004 *J. Alloy. Compd.* **368** 308
[9] Tian Z X, Xiao W, Wan F R and Geng W T 2010 *J. Nucl. Mater.* **407** 200
[10] Wu R, Freeman A J and Olson G B 1994 *Science* **265** 376
[11] Zhang Y, Feng W Q, Liu Y L, Lu G H and Wang T M 2009 *Nucl. Instrum. Meth. B* **267** 3200
[12] Hristova E, Janisch R, Drautz R and Hartmaier A 2011 *Comput. Mater. Sci.* **50** 1088
[13] Gesari S, Irigoyen B and Juan A 2006 *Appl. Surf. Sci.* **253** 1939
[14] Birnbaum H K and Sofronis P 1994 *Mater. Sci. Eng. A* **176** 191
[15] Lassila D H and Birnbaum H K 1987 *Acta Metall.* **35** 1815
[16] Kim S, Kim S G, Horstemeyer M F and Rhee H 2012 arXiv:1201.5915
[17] Čák M, Šob M and Hafner J 2008 *Phys. Rev. B* **78** 054418
[18] Shang J X and Wang C Y 2001 *J. Phys.: Condens. Matter* **13** 9635
[19] Shang J X, Zhao X D, Wang F H, Wang C Y and Xu H B 2006 *Comput. Mater. Sci.* **38** 217
[20] Yeşilleten D, Nastar M, Arias T A, Paxton A T and Yip S 1998 *Phys. Rev. Lett.* **81** 2998
[21] Wu R, Freeman A J and Olson G B 1996 *Phys. Rev. B* **53** 7504
[22] Wachowicz E, Ossowski T and Kiejna A 2010 *Phys. Rev. B* **81** 094104
[23] Bhattacharya S K, Tanaka S, Shiihara Y and Kohyama M 2013 *J. Phys.: Condens. Matter* **25** 135004
[24] Ossowski T, Wachowicz E and Kiejna A 2009 *J. Phys.: Condens. Matter* **21** 485002
[25] Hohenberg P and Kohn W 1964 *Phys. Rev. B* **136** 864
[26] Kohn W and Sham L J 1965 *Phys. Rev.* **140** A1133
[27] Payne M C, Teter M P, Allan D C, Arias T A and Joannopoulos J D 1992 *J. Mod. Phys*. **64** 1045
[28] Vanderbilt D 1990 *Phys. Rev. B* **41** 7892
[29] Monkhorst H J and Pack J D 1976 *Phys. Rev. B* **13** 5188
[30] Perdew J P, Burke K and Ernzerhof M 1996 *Phys. Rev. Lett.* **77** 3865
[31] Griffith A A 1921 *Philos. T. Roy. Soc. A* **221** 163
[32] Yang R, Zhao D L, Wang Y M, Wang S Q, Ye H Q and Wang C Y 2001 *Acta Mater.* **49** 1079
[33] Yang R, Wang Y M, Ye H Q and Wang C Y 2001 *J. Phys.: Condens. Matter* **13** 4485
[34] Messmer R P and Briant C L 1982 *Acta Metall.* **30** 457
[35] Seah M P 1975 *Surf. Sci.* **53** 168